FONDO EUROPEO DE
DESENVOLVEMENTO
REXIONAL
"Unha maneira de facer Europa"
UNIÓN EUROPEA

LFU tests in semileptonic decays at LHCb

Julio Nóvoa Fernández (IGFAE-USC)
on behalf of the LHCb collaboration

L International Meeting on Fundamental Physics and XV CPAN Days
2 October 2023

LHCb
IGFAE Instituto Galego de Física de Altas Enerxías
USC Universidade de Santiago de Compostela
XUNTA DE GALICIA
galicia

Outline

1. Introduction to Lepton Flavour Universality (LFU)
2. Latest LFU results at LHCb
    1. Angular observables: first LHCb measurement of F_L^{D*} fraction
    2. Ratio observables: LHCb measurements of $R(D) - R(D*)$ muonic and $R(D*)$ hadronic
3. Current status of LFU tests at IGFAE
    1. Simultaneous measurement of $R(D^0) - R(D^{*0})$ hadronic
    2. Measurement of $R(D*)$ hadronic with $D^{*-} \to \pi^- \bar{D}^0(\to K^+\pi^-\pi^+\pi^-)$ decays
4. Conclusions and prospects

Lepton Flavour Universality (LFU)

- In SM, there are 3 families of leptons.
- LFU: equal EW couplings between gauge bosons and every lepton (when their mass differences are accounted for).
- Experimental measurements suggest possible LFU violations.
- These deviations could be produced by NP: charged Higgs, leptoquarks…?
- Two main methods to probe LFU at LHCb: ratio observables and angular analyses.

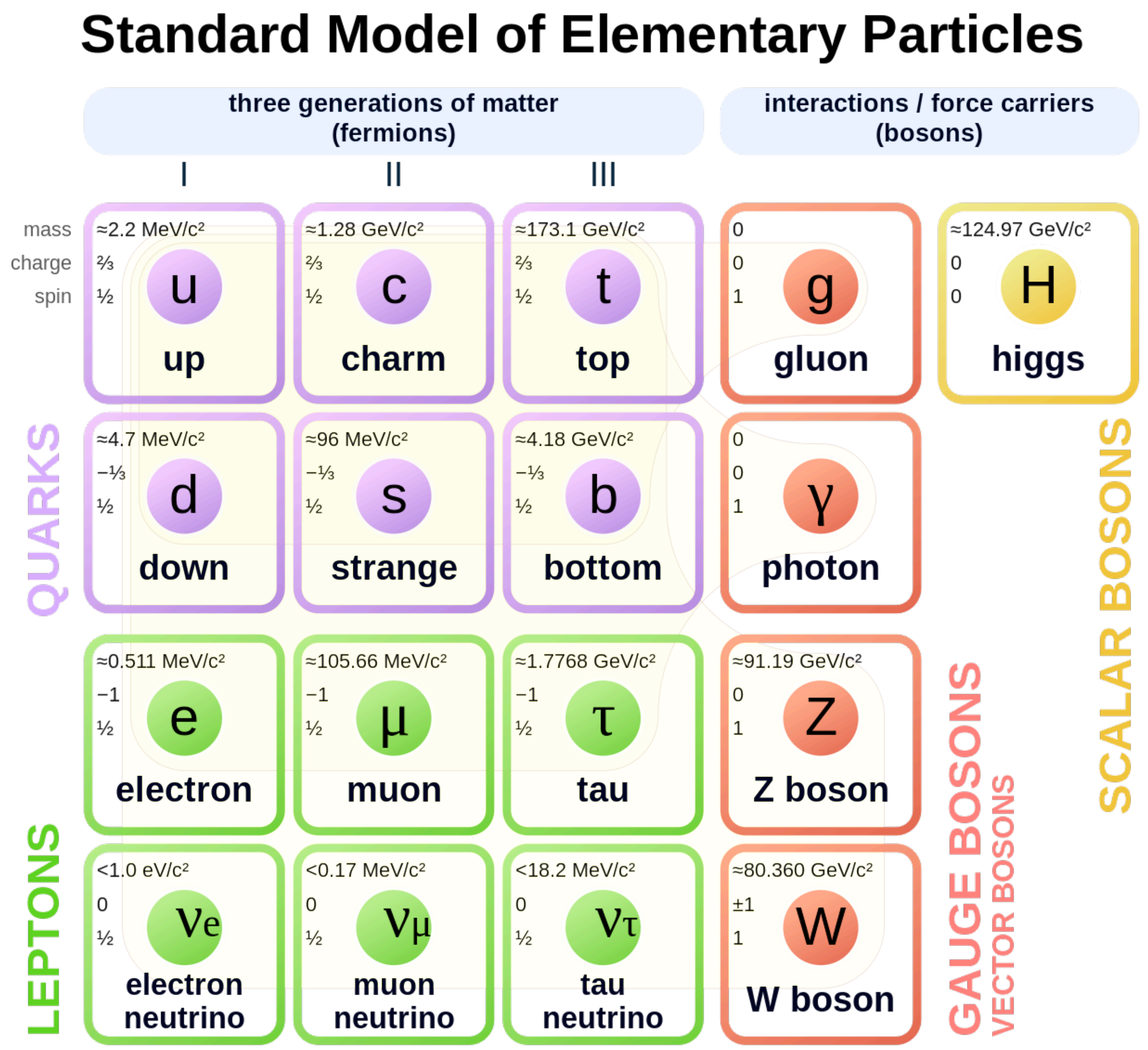

Angular analyses in $B \to D^* \tau \nu$ decays

- LFU ratios arise from fully integrated BR.
- Angular fractions are partially integrated, so they provide additional information.
- Signal may be divided into an unpolarised fraction $a_{\theta_D}(q^2)$ and a polarised fraction $c_{\theta_D}(q^2)$ as functions of $q^2 = (p_B - p_{D^*})^2$.
- The longitudinal polarisation fraction is defined as:

$$F_L^{D^*} = \frac{a_{\theta_D}(q^2) + c_{\theta_D}(q^2)}{3a_{\theta_D}(q^2) + c_{\theta_D}(q^2)}$$

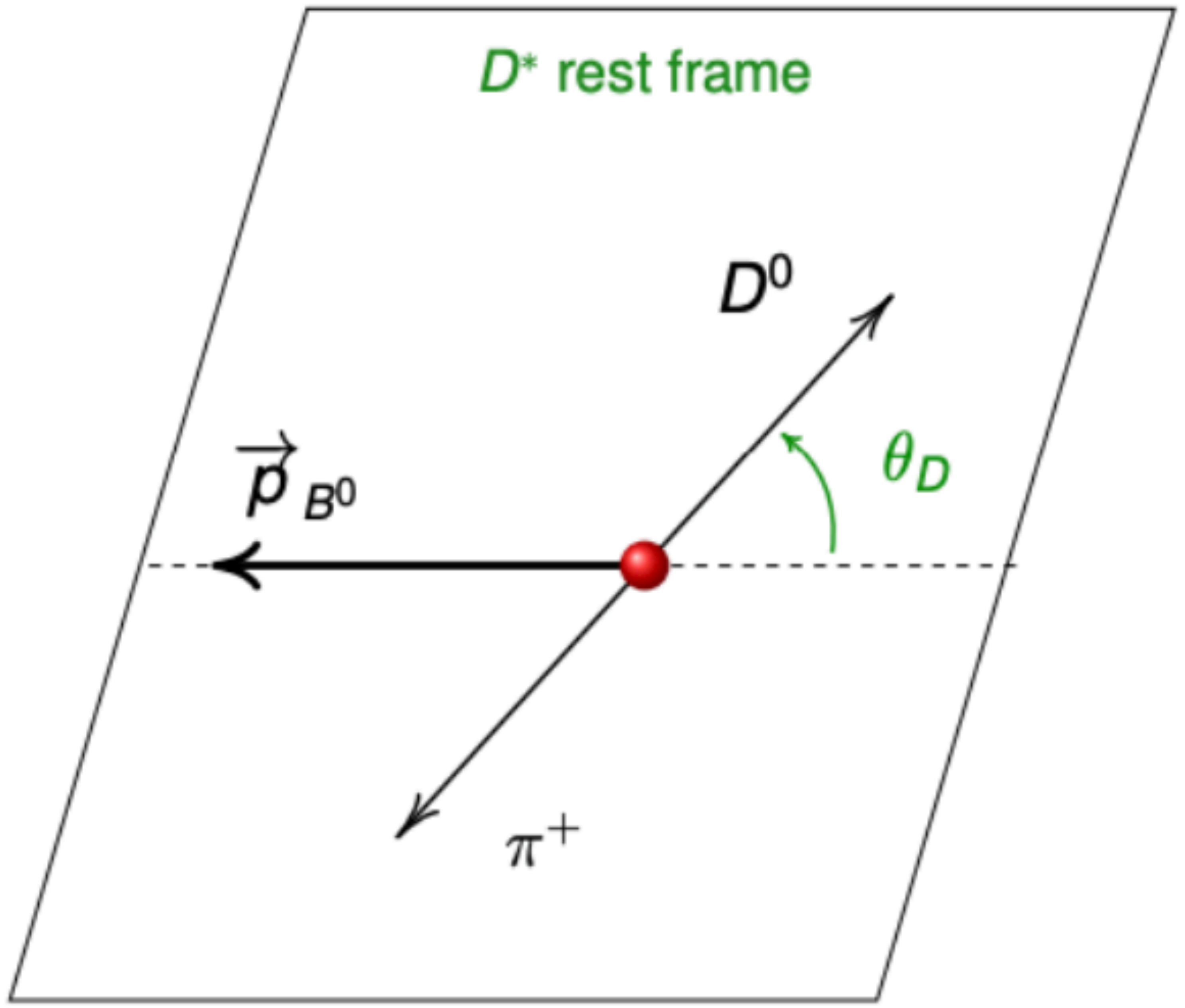

SM prediction:
$F_L^{D^*} = 0.441 \pm 0.006$
Phys. Rev. D 98, 095018 (2018)

Belle (2018):
$F_L^{D^*} = 0.60 \pm 0.08 \pm 0.04$

LHCb results on F_L^{D*} polarisation fraction

- Simultaneous 4D fit to Run-1+Run-2 data in two q^2 regions around 7 GeV$^2/c^4$.
- Fit variables: $q^2, \cos\theta_D, \tau$ decay time and BDT output.
- Results:

$$q^2 < 7\ \text{GeV}^2/c^4 : F_L^{D*} = 0.51 \pm 0.07\ \text{(stat)} \pm 0.03\ \text{(syst)}$$
$$q^2 > 7\ \text{GeV}^2/c^4 : F_L^{D*} = 0.35 \pm 0.08\ \text{(stat)} \pm 0.02\ \text{(syst)}$$
$$q^2\ \text{integrated} : F_L^{D*} = 0.43 \pm 0.06\ \text{(stat)} \pm 0.03\ \text{(syst)}$$

- Compatible with SM predictions $< 1\sigma$.
- Paper in preparation.

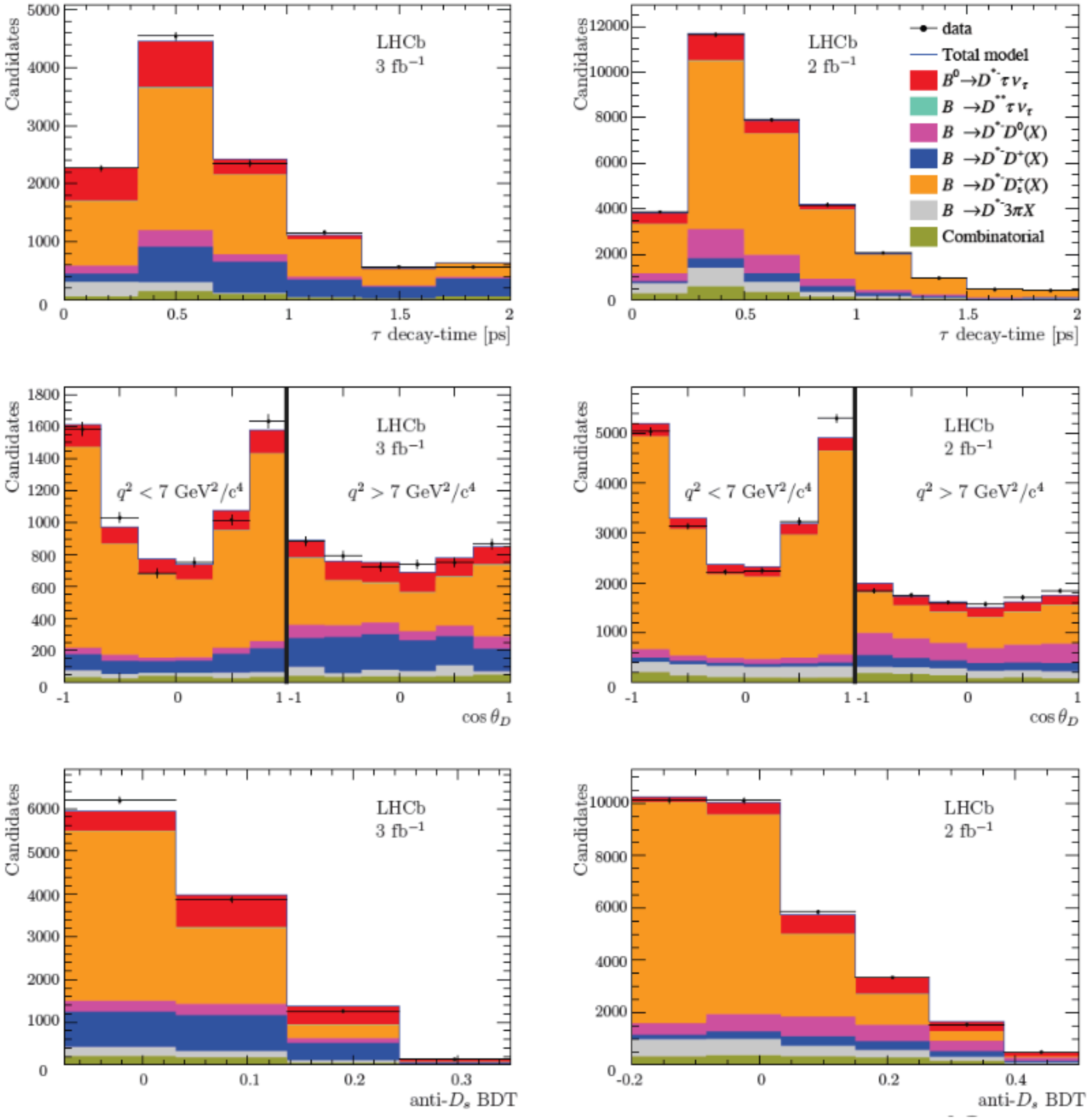

Ratio observables

$$R(D^{(*)}) = \frac{BR(B^0 \to D^{(*)}\tau^+\nu_\tau)}{BR(B^0 \to D^{(*)}\mu^+\nu_\mu)}$$

- Accurate SM theoretical predictions (hadronic uncertainties cancel out).
- Experimental systematic uncertainties are reduced as well (eff. quotient).
- Other ratios are also studied, e.g. *R(*Λ_c^+*)*, *R(*J/ψ*)* etc.
- Two general strategies for the reconstruction of tau:
    - Muonic: $\tau^+ \to \mu^+\bar{\nu}_\mu\nu_\tau$
    - Hadronic: $\tau^+ \to \pi^+\pi^-\pi^+\nu_\tau$

Signal and normalisation

- Hadronic ratios are usually redefined by introducing a normalisation channel:

$$R(D^*) = \frac{\mathcal{B}(B^0 \to D^{*-}\tau^+\nu_\tau)}{\mathcal{B}(B^0 \to D^{*-}\pi^+\pi^-\pi^+)} \cdot \frac{\mathcal{B}(B^0 \to D^{*-}\pi^+\pi^-\pi^+)}{\mathcal{B}(B^0 \to D^{*-}\mu^+\nu_\mu)}$$

- The second fraction requires external inputs, while the first (hadronic) fraction is computed with yields and efficiencies:

$$R_{had}(D*) = \frac{N_{sig}}{N_{norm}} \cdot \frac{\epsilon_{norm}}{\epsilon_{sig}}$$

- Yields are estimated with 3D template fits and efficiencies are extracted from simulated samples.

Muonic and hadronic strategies

Muonic

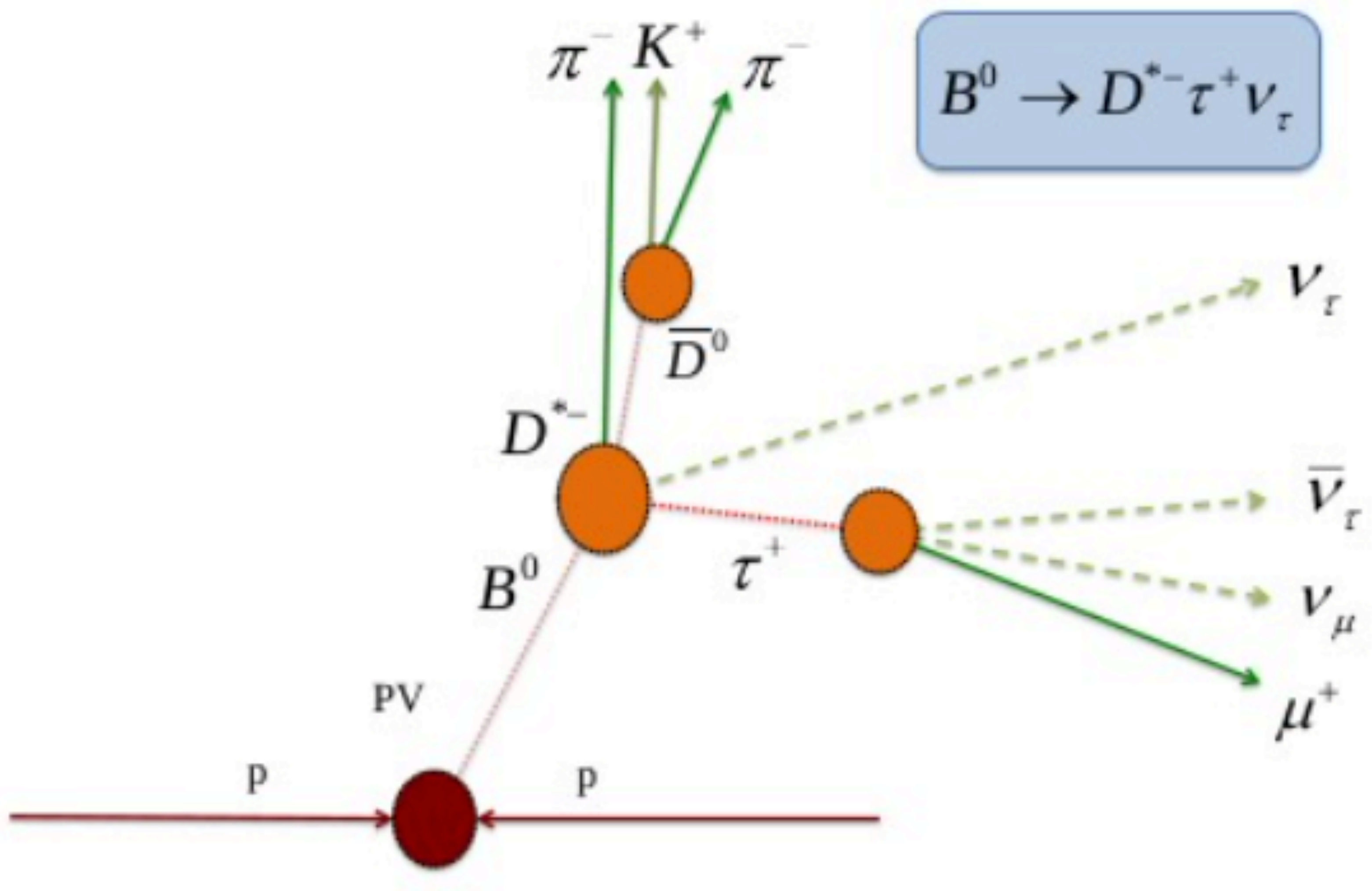

- Pros: direct measurement of the ratio, higher BR.
- Cons: significant background from partially-reconstructed decays.

Hadronic

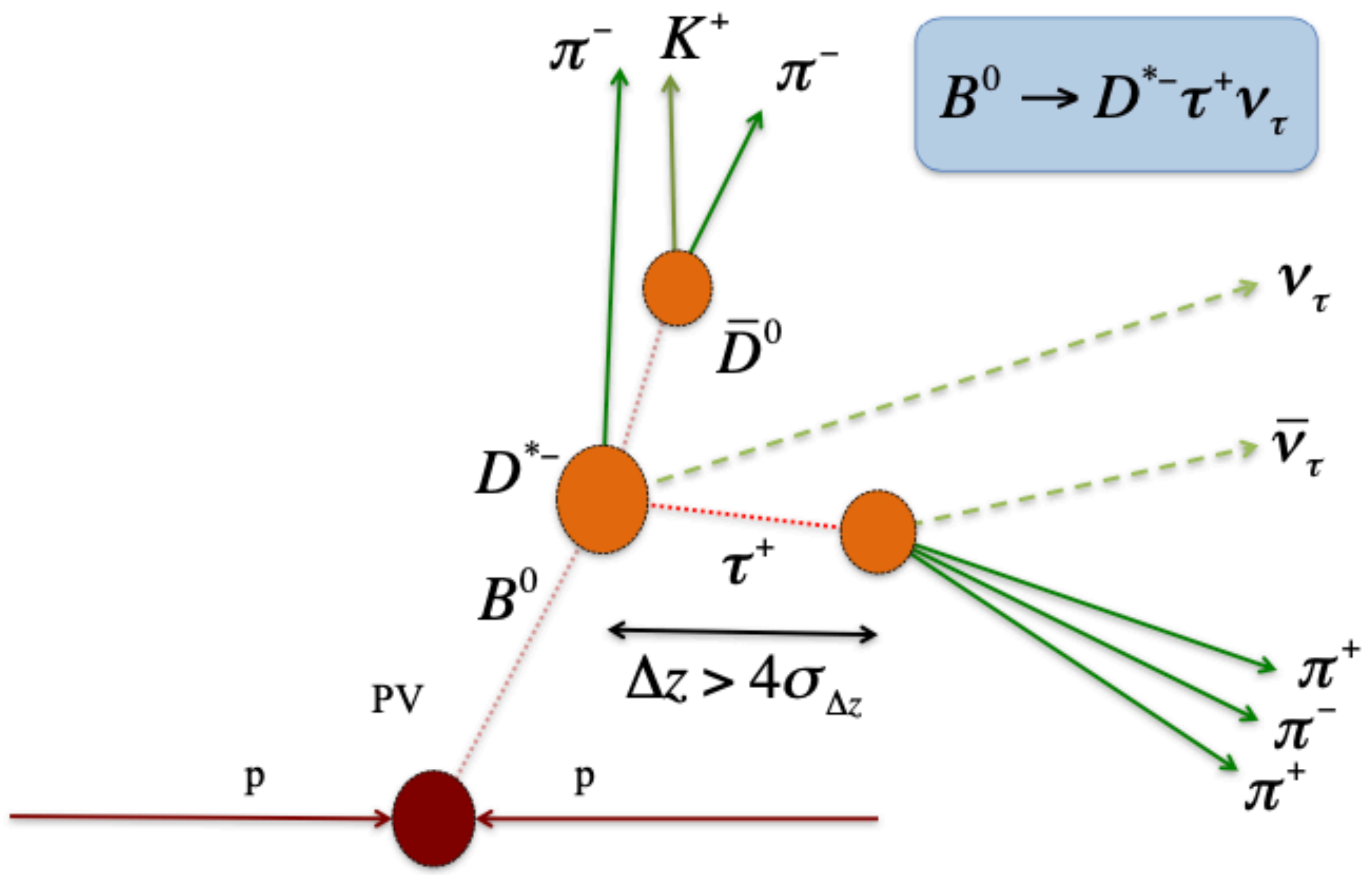

- Pros: higher background suppression, high purity samples.
- Cons: external inputs, lower BR.

$R(D) - R(D^*)$ world average

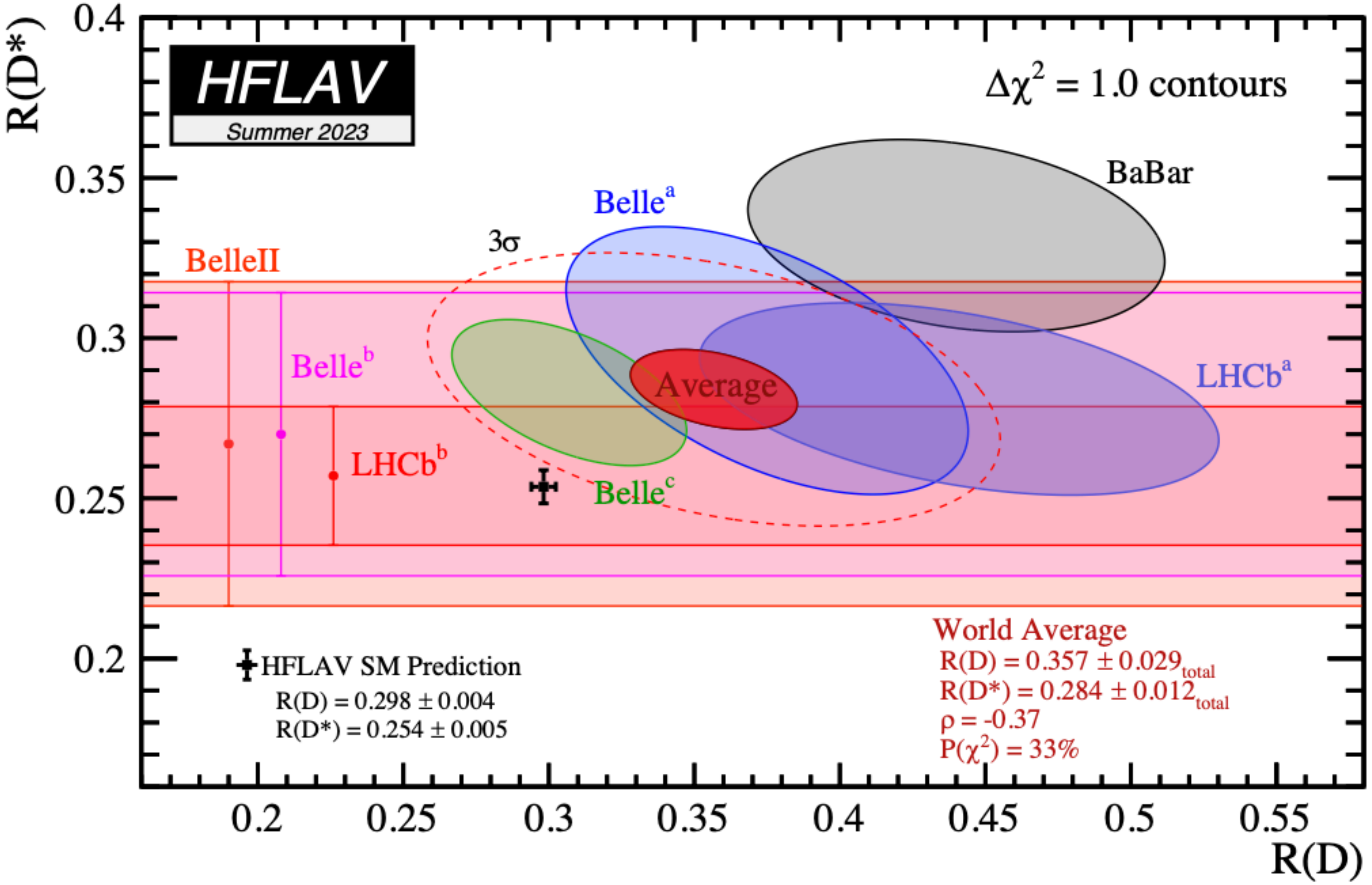

- *R(D)* and *R(D*)* deviate from SM predictions by 2.0σ and 2.2σ, respectively.
- Combined tension stands at $\sim 3.3\sigma$

LHCb results on $R(D) - R(D^*)$ muonic

- Simultaneous measurement of $R(D) - R(D^*)$, using Run-1 data.
- Muonic strategy, using $D^0\mu^-$ and $D^{*+}\mu^-$ candidates.
- 3D template fit on q^2, E^*_μ and $m^2_{miss} = (p_B - p_D - p_\mu)^2$ in 4 regions within the interval $q^2 \in [-0.4, 12.6]$ GeV$^2/c^4$
- Results in agreement with SM within 1.9σ.
- Phys. Rev. Lett. 131, 111802 (2023)

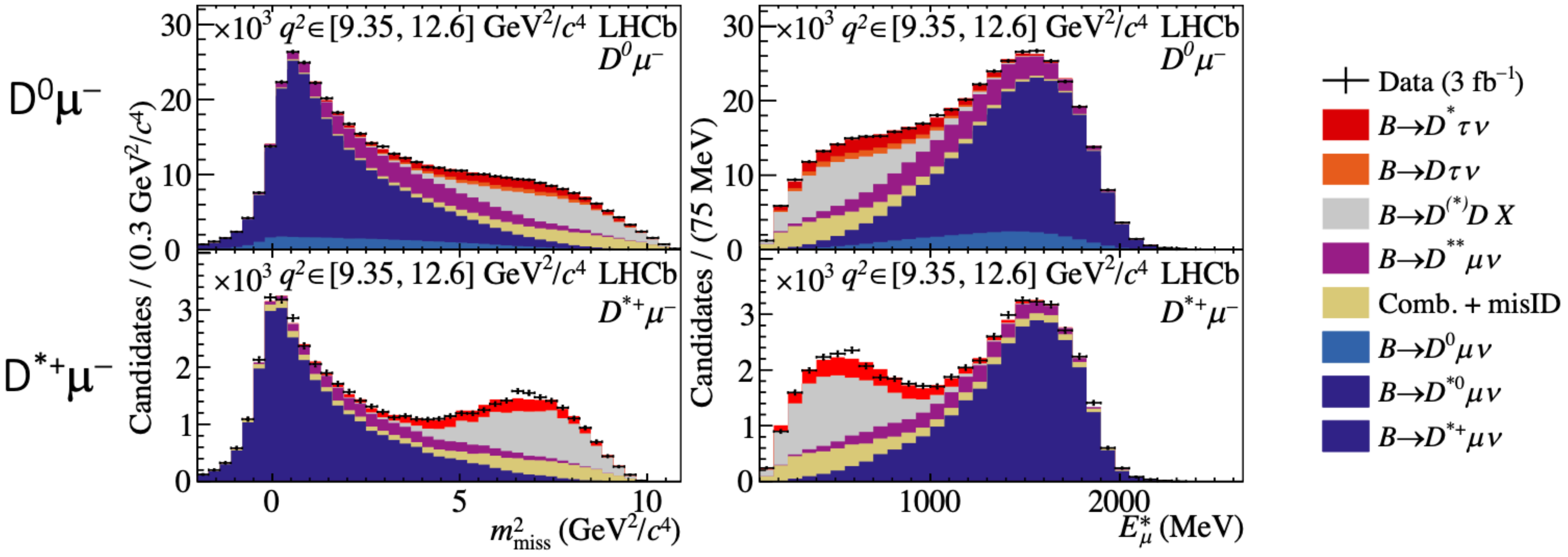

$R(D^*) = 0.81 \pm 0.018$ (stat) ± 0.024 (syst)

$R(D^0) = 0.441 \pm 0.060$ (stat) ± 0.066 (syst)

$\rho = -0.43$

LHCb results on $R(D^*)$ hadronic

- 3D fit to Run-2 data, using hadronic modes for tau reconstruction and $D^{*-} \to \bar{D}^0 \pi^-$ decays.
- 3D fit variables: q^2, τ decay time and BDT output.
- 1D fit for normalisation on $m(D^{*-}3\pi)$.
- Results:

$R(D^*) = 0.247 \pm 0.015$ **(stat)** $\pm\, 0.015$ **(syst)** $\pm\, 0.012$ **(ext)**

Combined with LHCb Run-1 hadronic result

(Phys. Rev. D 97,07219)

$R(D^*) = 0.257 \pm 0.012$ **(stat)** $\pm\, 0.014$ **(syst)** $\pm\, 0.012$ **(ext)**

- Agreement with world average, SM excess $\sim 1\sigma$.
- Phys. Rev. D108 012018 (2023)

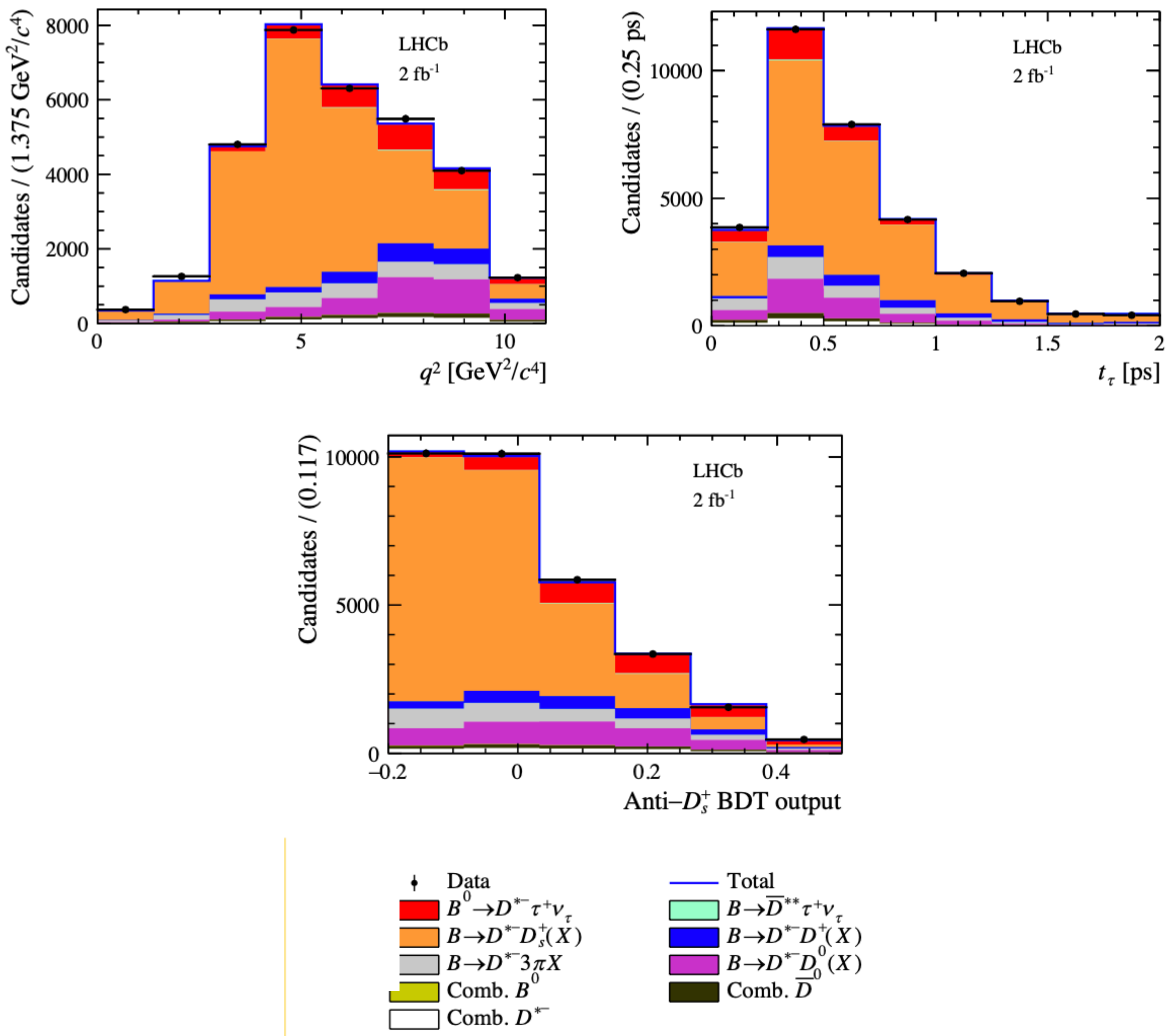

Measurement of $R(D^0) - R(D^{*0})$ hadronic at IGFAE

- Simultaneous measurement of $R(D^0) - R(D^{*0})$, using the 3-prong hadronic tau strategy and LHCb Run-2 data (2016-18).
- Selection of $D^0 \to K^+\pi^-$ and $D^{*0} \to D^0\pi^0$ or $D^{*0} \to D^0\gamma$ decays.
- Norm. channel: $B^- \to D^0 D_s^-(\to 3\pi)$
- Analysis already under LHCb internal review (results are still blinded).
- Paper draft in preparation.

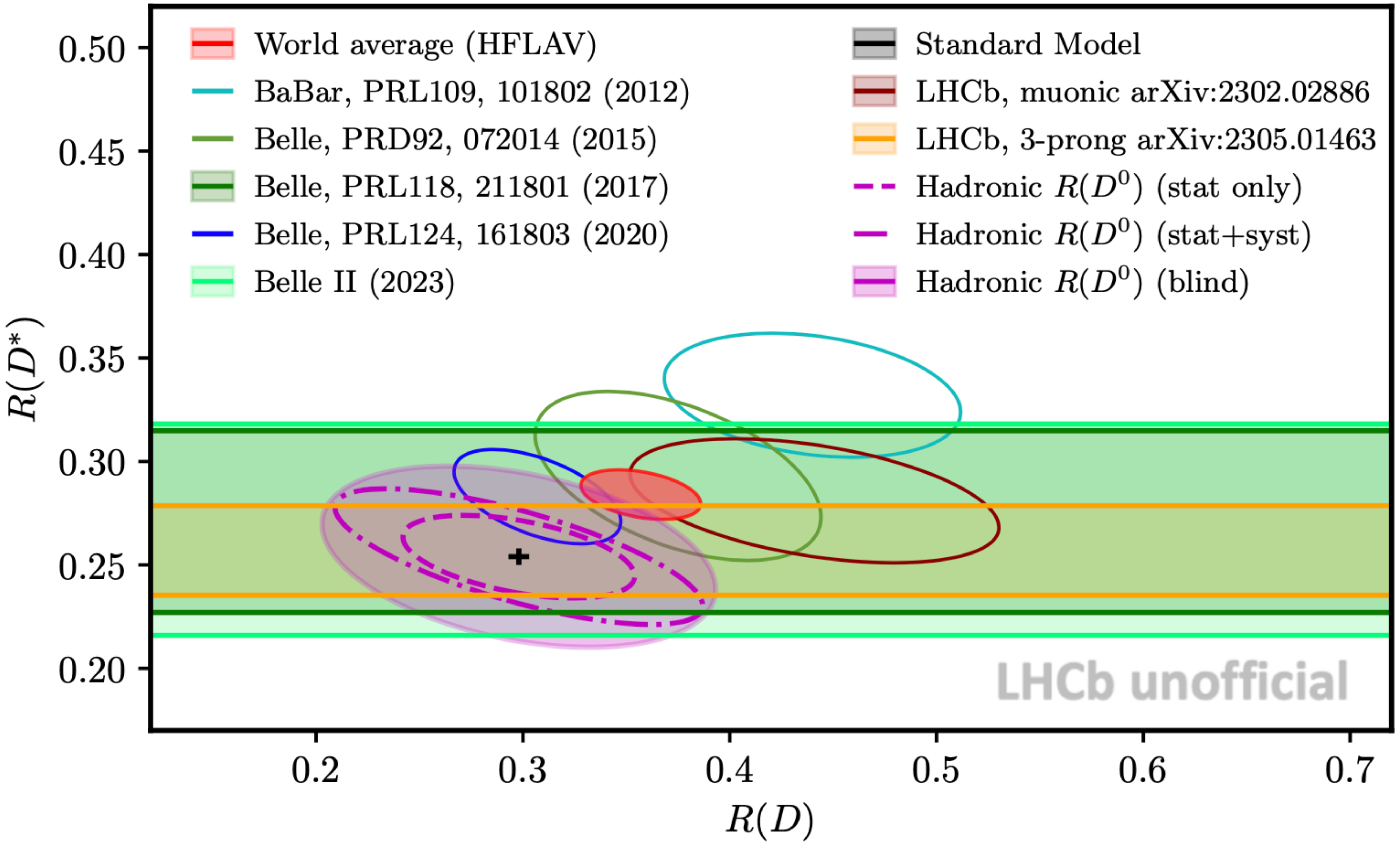

Measurement of $R(D^{*-})$ hadronic at IGFAE

- Novel approach for the measurement of $R(D^{*-})$, using $D^{*-} \to D^0\pi^-$ and $D^0 \to K^+\pi^-\pi^+\pi^-$decays (instead of $K^+\pi^-$, as in previous analyses).
- Hadronic tau reconstruction.
- LHCb Run-2 data analysis (2016-18).
- Latest progress: MC production, efficiency computation, control-sample studies to model background processes.
- Next steps: implementation of 2D and 3D fit models to estimate signal and normalisation yields.

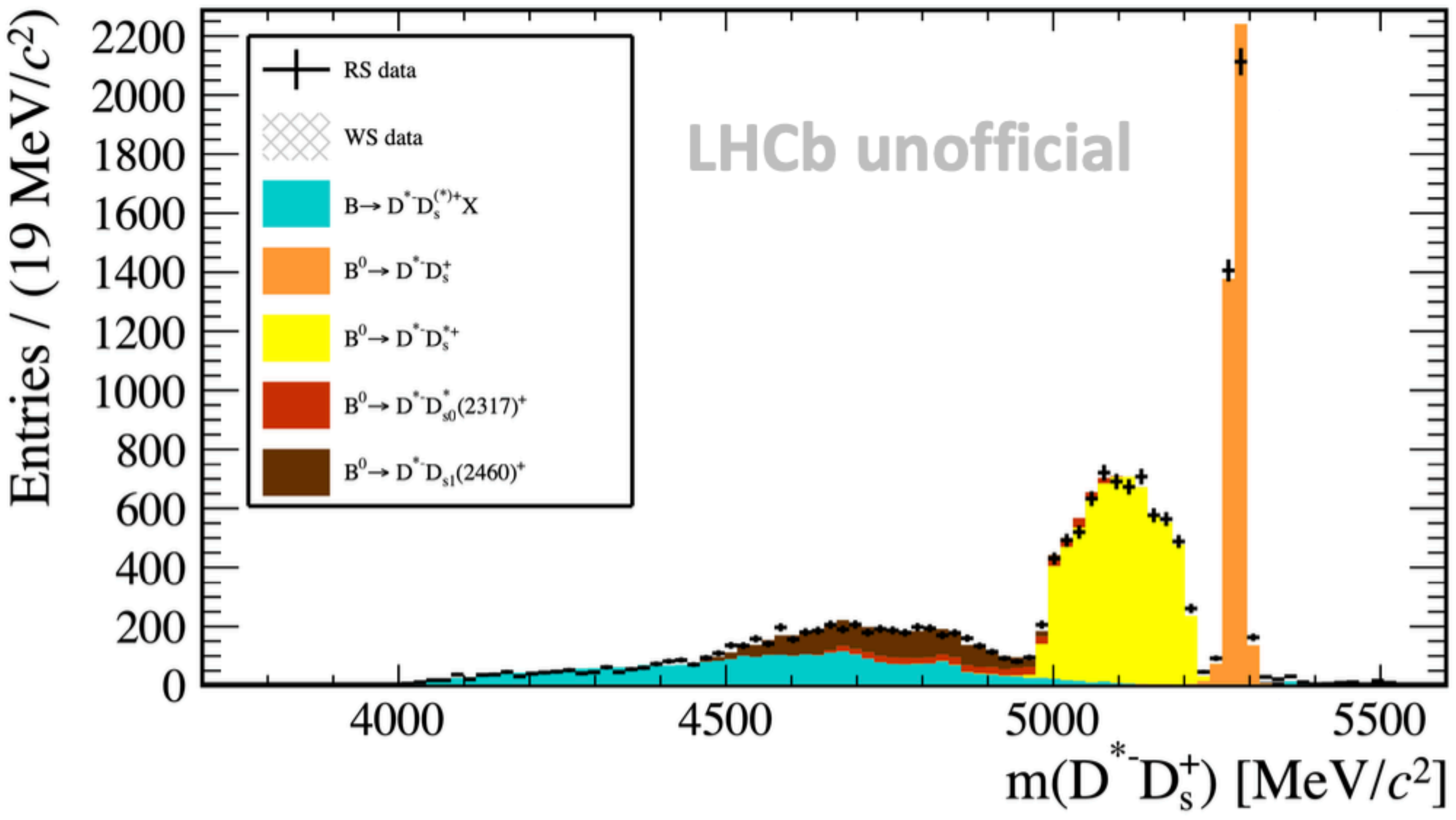

Conclusions and prospects

- New LHCb measurements of $R(D) - R(D^*)$ muonic and $R(D^*)$ hadronic.
  - Combined tension is around 3.3σ.
- First LHCb measurement of $F_L^{D^*}$ polarisation fraction.
  - Accurate result, compatible with SM.
- More LFU results are needed to solve the current disagreement.
  - Several $R(D^{(*)})$ tests are being developed at LHCb (also at IGFAE).
  - Other ongoing LHCb studies: full angular analyses, further measurements of $R(X_c)$ with different charm mesons.

Optimistic projection

- LHC Run 3 will provide large data samples to analyse in the near future.
- Uncertainties for ratio observables are expected to decrease significantly for Run 3 samples and beyond.
- PRD 94 (2022) 015003

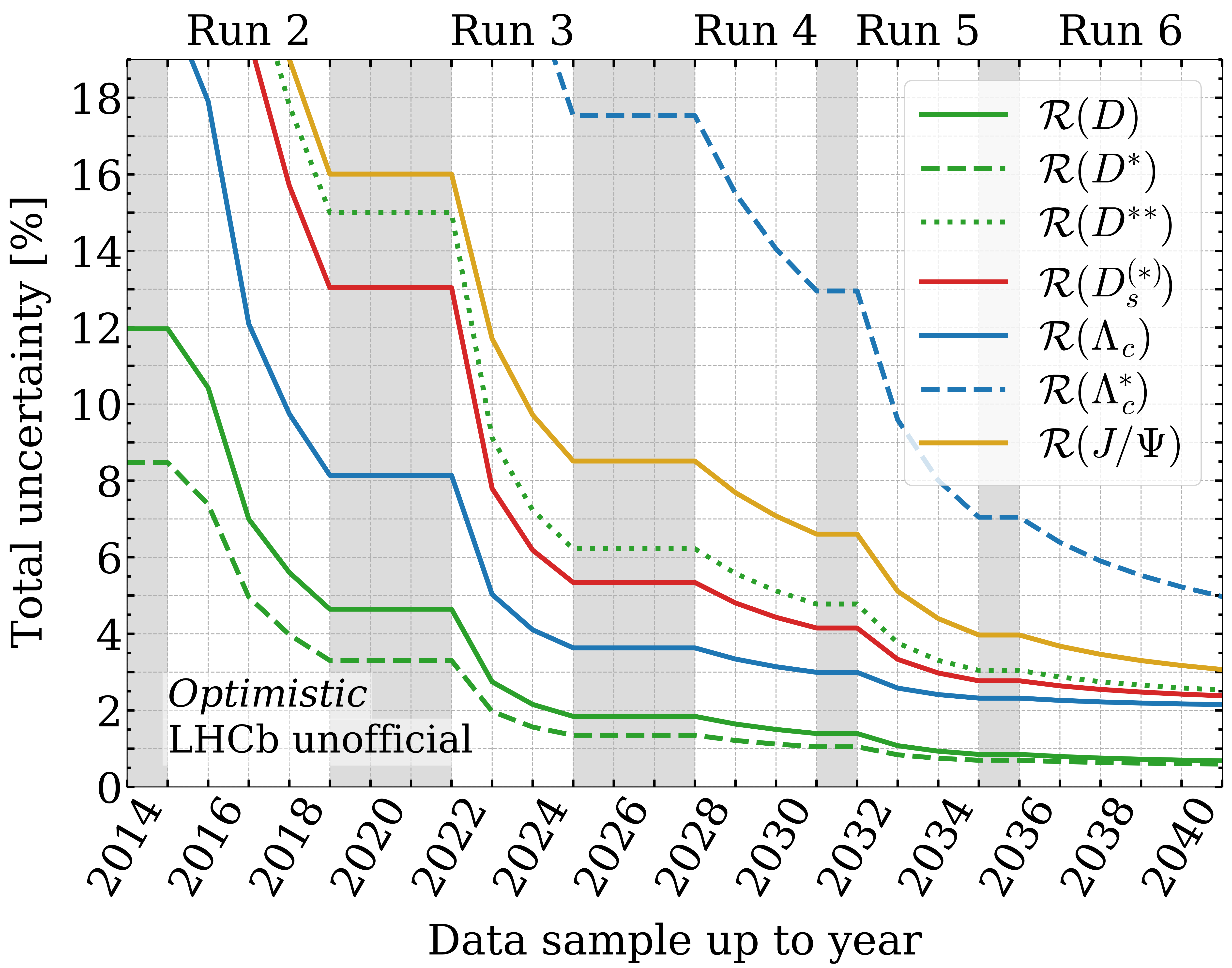

Thank you for your attention!

BACKUP

LHCb experiment

- Single-arm forward detector, designed for high-precision studies of *b* and *c* hadron physics ($\sim 25\,\%\ b\bar{b}$ pairs are within LHCb acceptance).
- Excellent PID:
    - $\epsilon(K) \approx 95\,\%$
    - $\epsilon(\mu) \approx 95\,\%$
- High momentum, spatial and time resolutions:
    - $\sigma_p/p \approx 0.4 - 0.6\,\%\,(5 - 100\,\text{GeV}/c)$
    - $\sigma_{IP} \approx 20\,\mu\text{m}$ (at high p_T)
    - $\sigma_t \approx 50\,\text{fs}$

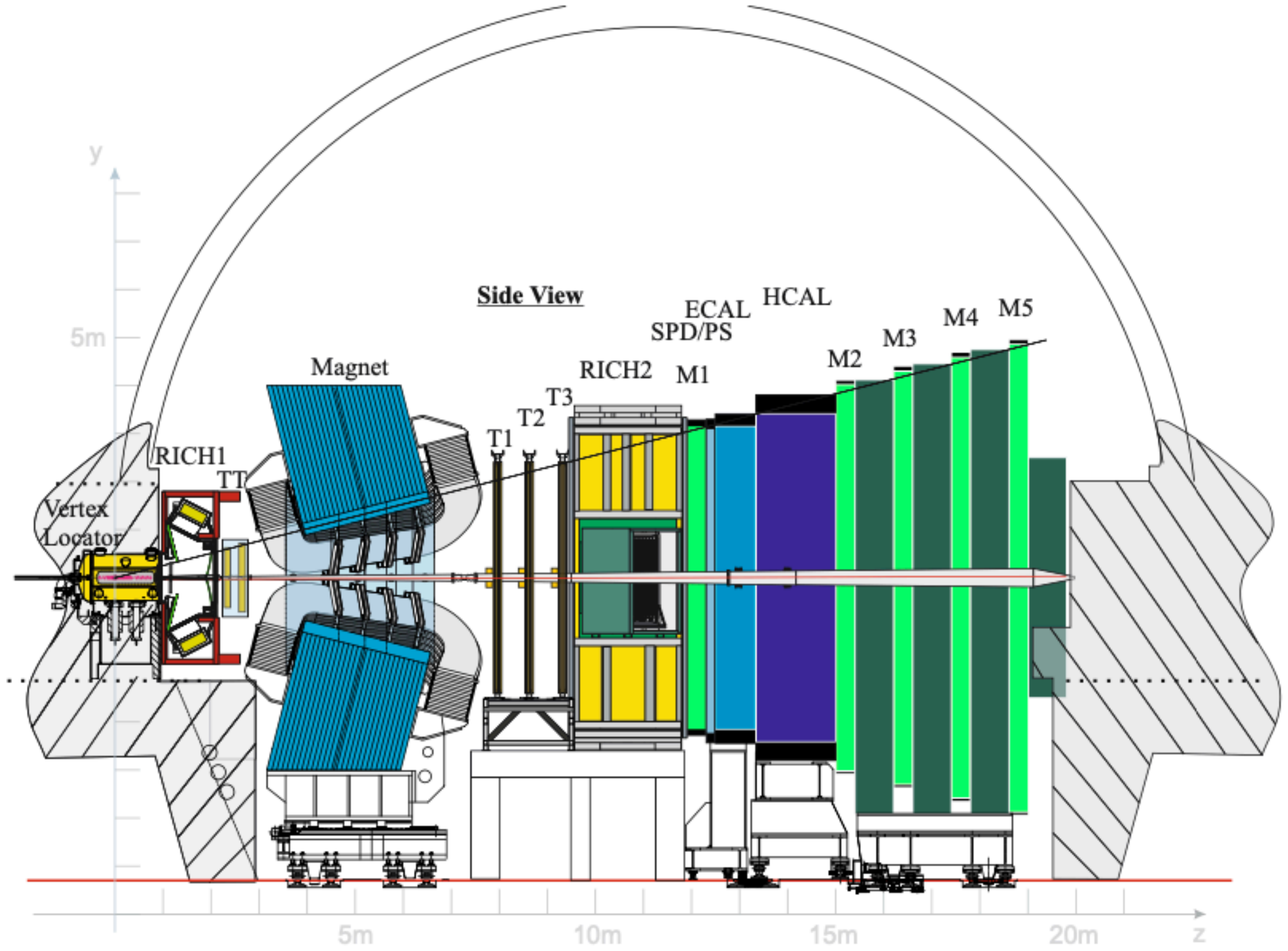

LHCb collected data

- Run 1 (2010-2012):
  - $\sqrt{s} \approx 7.8$ TeV
  - ~ 3 fb^{-1}
- Run 2 (2015-2018):
  - $\sqrt{s} \approx 13$ TeV
  - ~ 6 fb^{-1}
- Run 3 (2022-present)

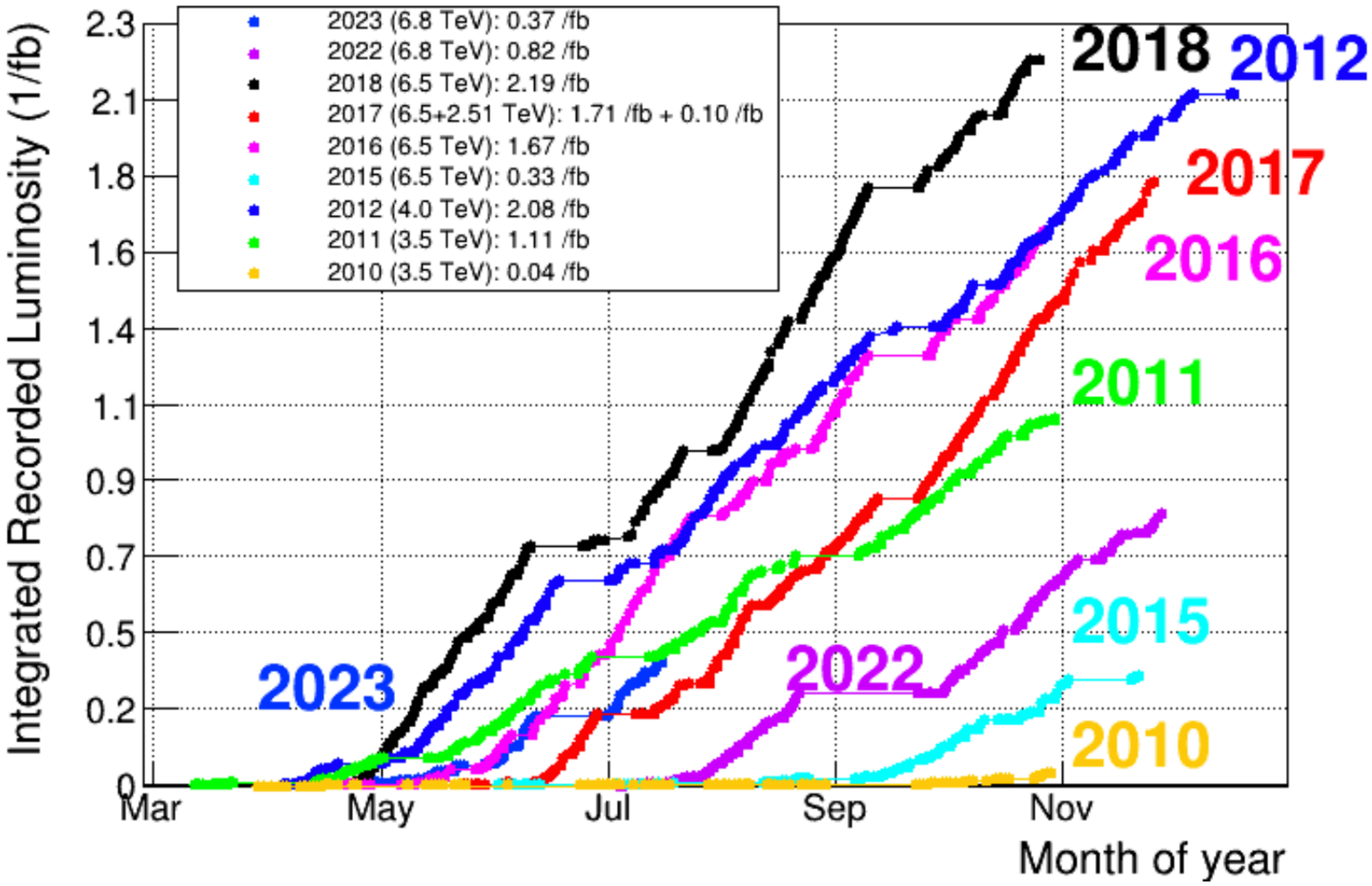

$F_L^{D^*}$ fraction in $B \to D^*\tau\nu$ decays - syst. uncertainties

Source	low q^2	high q^2	integrated
Fit validation	0.003	0.002	0.003
FF model	0.007	0.003	0.005
FF parameters	0.013	0.006	0.011
TemplateSize	0.027	0.017	0.019
fSignal0	0.001	0.001	0.001
fSignalDstst	0.001	0.004	0.003
Signal selection	0.005	0.004	0.005
Bin migration	0.008	0.006	0.007
$F_L^{D^*}$ in simulation	0.007	0.003	0.007
D_s^+ decay model	0.008	0.009	0.009
$\cos\theta_D$ $D^{*-}D_s^+$	0.002	0.001	0.002
$\cos\theta_D$ $D^{*-}D_s^{*+}$	0.007	0.002	0.004
$\cos\theta_D$ $D^{*-}D_s^+X$	0.007	0.006	0.007
$\cos\theta_D$ $D^{*-}D^+X$	0.002	0.002	0.003
$\cos\theta_D$ $D^{*-}D^0X$	0.002	0.002	0.003
$F_L^{D^*}$ integrated	-	-	0.002
Total	0.036	0.023	0.029

- Main sources of systematic uncertainty:
    - Limited size of simulated samples.
    - Form factor parameterisation and modelling.

$R(D) - R(D^*)$ muonic - syst. uncertainties

Internal fit uncertainties	$\sigma_{\mathcal{R}(D^*)}(\times 10^{-2})$	$\sigma_{\mathcal{R}(D^0)}(\times 10^{-2})$
Statistical uncertainty	1.8	6.0
Simulated sample size	1.5	4.5
$B \to D^{(*)}DX$ template shape	0.8	3.2
$\overline{B} \to D^{(*)}\ell^-\overline{\nu}_\ell$ form-factors	0.7	2.1
$\overline{B} \to D^{**}\mu^-\overline{\nu}_\mu$ form-factors	0.8	1.2
$\mathcal{B}\ (\overline{B} \to D^* D_s^-(\to \tau^-\overline{\nu}_\tau)X)$	0.3	1.2
MisID template	0.1	0.8
$\mathcal{B}\ (\overline{B} \to D^{**}\tau^-\overline{\nu}_\tau\ )$	0.5	0.5
Combinatorial	< 0.1	0.1
Resolution	< 0.1	0.1
Additional model uncertainty	$\sigma_{\mathcal{R}(D^*)}(\times 10^{-2})$	$\sigma_{\mathcal{R}(D^0)}(\times 10^{-2})$
$B \to D^{(*)}DX$ model uncertainty	0.6	0.7
$\overline{B}{}_s^0 \to D_s^{**}\mu^-\overline{\nu}_\mu$ model uncertainty	0.6	2.4
Data/simulation corrections	0.4	0.8
Coulomb correction to $\mathcal{R}(D^{*+})/\mathcal{R}(D^{*0})$	0.2	0.3
MisID template unfolding	0.7	1.2
Baryonic backgrounds	0.7	1.2
Normalization uncertainties	$\sigma_{\mathcal{R}(D^*)}(\times 10^{-2})$	$\sigma_{\mathcal{R}(D^0)}(\times 10^{-2})$
Data/simulation corrections	$0.4 \times \mathcal{R}(D^*)$	$0.6 \times \mathcal{R}(D^0)$
$\tau^- \to \mu^-\nu\overline{\nu}$ branching fraction	$0.2 \times \mathcal{R}(D^*)$	$0.2 \times \mathcal{R}(D^0)$
Total systematic uncertainty	2.4	6.6
Total uncertainty	3.0	8.9

- Main sources of systematic uncertainty:
  - Limited size of simulated samples.
  - Shape parameters from control region.

$R(D^*)$ hadronic - syst. uncertainties

Source	Systematic uncertainty (%)
Signal decay template shape	1.8
Signal decay efficiency	0.9
Fractions of signal τ^+ decays	0.3
Possible contributions from other τ^+ decays	1.0
Fixing the $\bar{D}^{**}\tau^+\nu_\tau$ and $D_s^{**+}\tau^+\nu_\tau$ fractions	$^{+1.8}_{-1.9}$
Normalization mode PDF choice	1.0
Knowledge of the $D_s^+ \to 3\pi X$ decay model	1.0
Specifically the $D_s^+ \to a_1 X$ fraction	1.5
$B \to D^{*-}D_s^+(X)$ template shapes	0.3
$B \to D^{*-}D^0(X)$ template shapes	1.2
$B \to D^{*-}D^+(X)$ template shapes	$^{+2.2}_{-0.8}$
Fixing $B \to D^{*-}D_s^+(X)$ background model parameters	1.1
Fixing $B \to D^{*-}D^0(X)$ background model parameters	1.5
$B \to D^{*-}3\pi X$ template shapes	1.2
Combinatorial background normalization	$^{+0.5}_{-0.6}$
PID efficiency	0.5
Kinematic reweighting	0.7
Vertex error correction	0.9
Normalization mode efficiency [modeling of $m(3\pi)$]	1.0
Preselection efficiency	2.0
Signal efficiency (size of simulation sample)	1.1
Normalization efficiency (size of simulation sample)	1.1
Empty bins in templates	1.3
PDF shapes uncertainty (size of simulation sample)	2.0
Total systematic uncertainty	$^{+6.2}_{-5.9}$
Total statistical uncertainty	5.9

- Main sources of systematic uncertainty:
  - Limited size of simulated samples.
  - Signal and background modelling.